ORIGINAL RESEARCH PAPER
Pages: 196-204

Microstrip Band-pass Filter with Adjustable Center Frequency and Fixed Bandwidth Property Using a Modified 3-Section SIR Resonator

F. Geran Gharakhili and A. Vaezi
Faculty of Electrical Engineering, Shahid Rajaee Teacher Training University, Tehran, Iran
f.geran@srttu.edu, ali_vaezi_ee@yahoo.com
Corresponding author: f.geran@srttu.edu

DOI:10.22070/JCE.2023.4981.1150

Abstract- This paper presents a novel microstrip bandpass filter (BPF), whose one of the most important feature of the filter is that the bandwidth remains fix as the center frequency changes. Therefore, the structure is suitable for reconfigurable communication systems. The BPF is consist of coupled-lines and a modify three section stepped impedance resonator (SIR) and a LPF that consists of one open-ended stub to suppress spurious harmonics at high frequencies. Even and odd mode analysis has been used for designing process of the BPF. Finally, the proposed filter has a fractional bandwidth of 25% at 3.095 GHz with the insertion loss less than 0.1 dB/ 3.715 dB in the pass-band (simulation/measurement), compact size, low insertion loss, right out of band rejection, high-frequency selectivity. The BPF is fabricated and measured. The excellent agreement between the measured and simulated results demonstrates the validity of the proposed filter and method.

Index Terms- Index Terms- Even and odd mode, adjustable center frequency, fixed bandwidth, modified 3-section stepped impedance resonator (SIR).

I. INTRODUCTION

As known, one of the most important element a microwave and millimeter-wave transceiver systems are filters. In the RF filter design, low insertion loss, high selectivity, wide stop-band and compact size are in high demand [1]. In the implementation microwave and millimeter-wave filters, planar technology such as microstrip, coplanar waveguide and, etc. are good candidates in the low-power systems. Various microstrip structures and resonators such as defected ground structures (DGS), stepped impedance resonator (SIR), electromagnetic coupling, etc. have been used to achieve the features as mentioned above [2]−[13]. In [2], a low-pass and band-pass triplexer have been designed

Manuscript received 15-March-2021 and revised 11-May-2021, *P-ISSN: 2322-4088*
Accepted on 13- June-2021 *E-ISSN:2322-3936*

by using one low-pass and two band-pass filters. For improvement of the performance of the introduced structure, a slot was etched in ground plane (DGS) that leads to reasonable isolations among the three bands (better than 40 dB). In [3], using symmetrical and asymmetrical compact microstrip resonant cell (CMRC) as the resonator, narrow-band microstrip BPFs with low insertion loss and high harmonic rejection were designed. Another structure using both half and quarter wavelength resonators was proposed in [4]. By adjustment of transmission zeroes, the frequency selectivity and out of band rejection of the BPF have been improved. A hybrid tri-band band-pass filter with controllable transmission zeroes is proposed in [5]. Adjustable the central frequency and bandwidth have been the special features of this article. In [6], a dual-mode dual-band microstrip BPF was designed for independently tuned dual- pass-bands. The dual-mode resonator and varactor diodes were proposed to determine the odd and even mode resonant frequencies independently. In [7], a fully tunable multi-band BPF with transmission zeroes at both sides of pass-bands was proposed. It is based on a quasi-bandpass scheme and has a quasi-elliptic response with controllable center frequency and bandwidth. In [8], a dual-mode balun BPF was designed by using the hybrid microstrip/slotline transmission lines and has high selectivity. In this letter, a microstrip BPF was designed with remarkable specifications such as low insertion loss, ultra-wide stop-band, and high selectivity by use of a novel resonator with a parallel-coupled line was presented. In [19], an approach with a new configuration was proposed for designing an ultra-wideband band-pass filter that demonstrates double/single notch-bands using microstrip transmission lines without using any via-hole. The proposed scheme using two parallel stepped-impedance resonators (SIR) provides two paths with different electrical lengths. The wave's cancellation theory was used for realizing notch bands to develop the pass-band of the UWB BPF. Also, in [20], another scheme has been proposed to design dual notch band BPF based on the left/right-handed method by using via holes. A tunable dual-band band-pass microstrip filter were proposed in [20]. In [21], two pairs of quarter wavelength transmission line resonators and two band-stop structures was used to compose the open stubs. The operation band-pass frequencies are generated by a pair of coupled resonators. The first coupled resonator was fed via a tap coupled and the second was fed by using a coupling structure. The configurability of the band-pass and the attenuation of the harmonics were achieved by adjusting the electrical length of the resonators and open stubs. This work is done by using a varactor diode capacitors. In [21], multilayer liquid crystal polymer (LCP) technology is used to design of the another UWB BPF scheme based on broadside coupled stepped impedance resonators. Also, embedding an open circuit stubs into broadside coupled stepped impedance resonators has created notch bands. The stepped impedance resonators are shown the behavior of harmonic suppression and, so, the proposed schemes have a high attenuation level and wide stop-band. In [17], a symmetric LPF was designed and analyzed by using of even and odd mode procedure. This method can be used to design the symmetric BPF.

Parameters' value of the designed filter is:
L1=0.3, L2=0.8,
L3=0.2, L4=10.3,
L5=0.2, L6=1.8,
L7=0.55, L8=1.5,
L9=0.55, L10=11.2,
L11=0.1, W1=5.8,
W2=7, W3=1,
W4=3.2, W5=2.1,
W6=0.65, W7=0.3,
W8=3 (All dimensions are in millimeter (*mm)*).

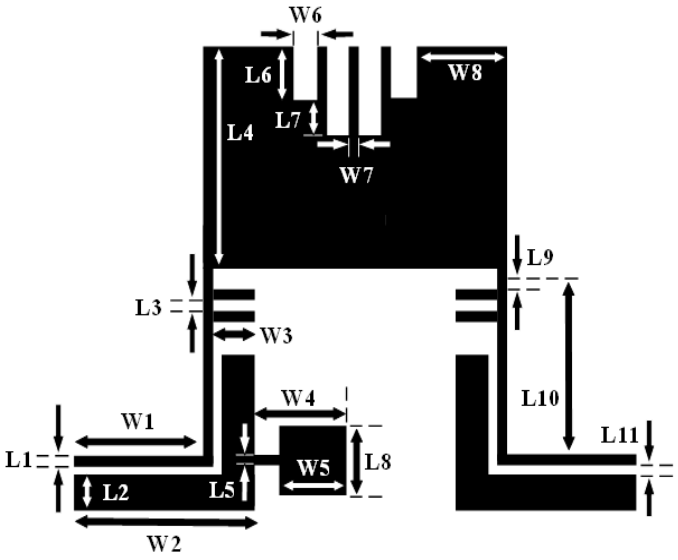

Fig. 1. The layout of the proposed BPF.

In this paper, a modify three section SIR for implementation of the BPF is presented. The initial value of the BPF dimensions are calculated by using of the even and odd mode analysis. One of the prominent features of the proposed filter is that the bandwidth remains fixed despite the change of the central frequency. Therefore, it would be a good option for designing a tunable filter. This paper is organized in four sections. Design procedure and analysis is given in section II. Section III is given fabrication and results. Finally, conclusion is presented in section IV.

II. DESIGN PROCEDURE AND ANALYSIS

The layout and dimensions of the proposed BPF are depicted in Fig. 1. A modified 3-section SIR based on the coupling theory has been selected as primary resonator. Since the structure of the primary resonator, as seen in Fig. 2, is symmetric, even and odd mode analysis is used to synthesize filter and optimize its performance. At odd mode (even mode) excitation, the voltage (current) is null along the T-T' line, which obtains the equivalent circuits are shown in Fig. 2. The microstrip line characteristic admittances and the electrical length have been symbolized by Yi (i=1-4) and θi (i=1-10), respectively. Also, Yi and θi are corresponded to the width and length of the microstrip line, respectively. Concerning the equivalent circuit of the even and odd mode, which is given in Fig. 2, the input admittance of the proposed filter at the odd and even mode is computed as follows:

Odd/even mode:

$$Y_{in,odd/even} = Y_1 \frac{Y_1^{o/e} + jY_1 \tan\theta_1}{Y_1 + jY_1^{o/e} \tan\theta_1} \quad (1)$$

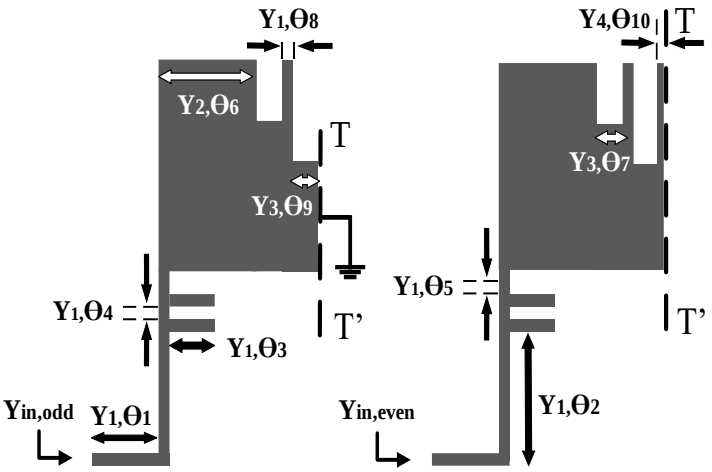

Fig. 2. Equivalent circuit of the main resonator. (a) Odd mode. (b) Even mode.

$$Y_1^{o/e} = Y_1 \frac{Y_2^{o/e} + jY_1 \tan\theta_2}{Y_1 + jY_2^{o/e} \tan\theta_2} \tag{2}$$

$$Y_m^{o/e} = jY_1 \tan\theta_3 + Y_1 \frac{Y_n^{o/e} + jY_1 \tan\theta_p}{Y_1 + jY_n^{o/e} \tan\theta_p} \quad m = 2,3 \;\; n = 3,4 \; and \;\; p = 4,5 \tag{3}$$

$$Y_m^{o/e} = Y_2 \frac{Y_n^{o/e} + jY_2 \tan\theta_p}{Y_2 + jY_n^{o/e} \tan\theta_p} \qquad m = 4,6 \; n = 5,7 \; and \;\; p = 6,8 \tag{5}$$

$$Y_5^o = Y_3 \frac{Y_6^o + jY_3 \tan\theta_7}{Y_3 + jY_6^o \tan\theta_7} \tag{6}$$

$$Y_7^o = -jY_4 \cot\theta_9 \text{ and } Y_7^e = jY_4 \tan\theta_9 \tag{8}$$

The resonance condition is equal to:

$Y_{in.odd}$ and $Y_{in.even} = 0 \; or \; \infty$

Where, the impedances of Y_1^(o/e) were calculated with the transmission line and open and short stubs relationships, step by step. The resonance condition is equal to Y_(in.odd) and Y_(in.even)=0 or ∞ "."

To extract the resonance frequencies of the odd and even mode, resonance condition is used. By changing the dimensions of the primary resonator, the odd and even mode resonance frequencies are adjustable. The effect of the physical length W1 in Fig. 1 that corresponds to θ1, on the odd and even mode resonances for three values of 2, 6 and 10 mm versus frequency is shown in Figs. 3(a) and 3(b).

As seen in Figs. 3(a) and 3(b), for larger values of W1, the odd and even mode resonance frequencies are moved to lower frequencies. Figs. 3(c) and 3(d) show the effect of physical length L10 in Fig.1 corresponds to θ2 on the odd and even mode resonance frequencies for three values of 7, 10 and, 13 mm.

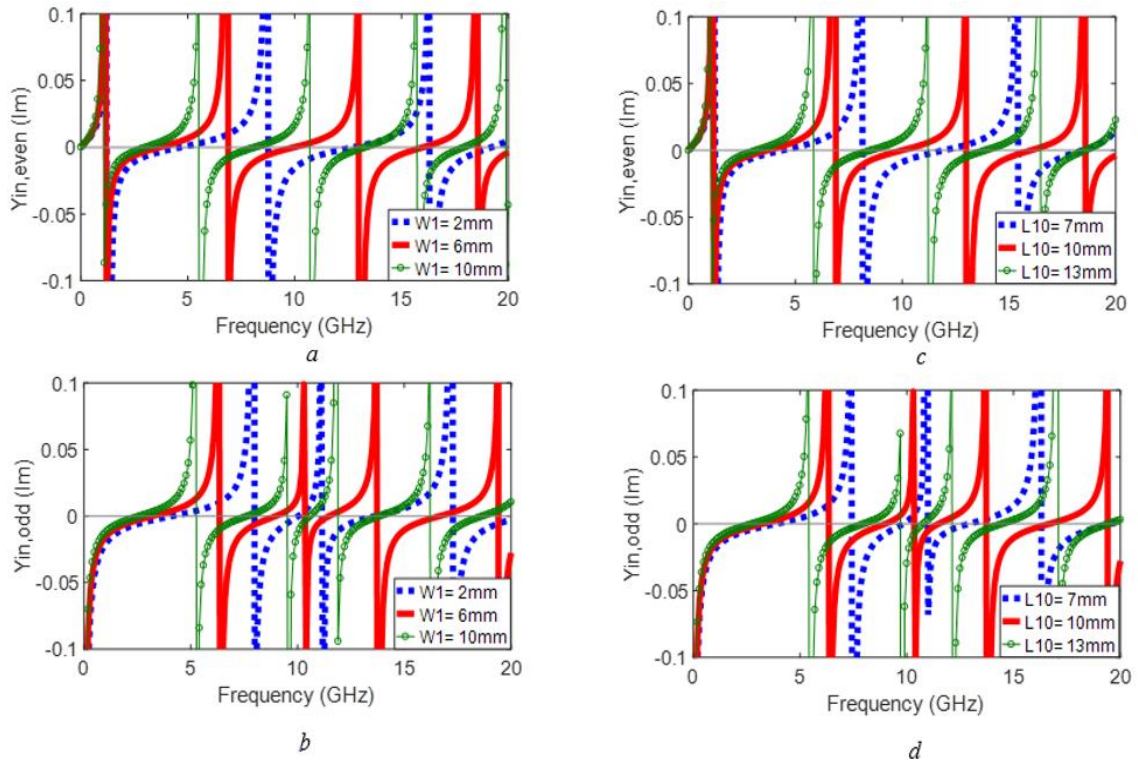

Fig. 3. The odd and even modes analysis. **(a)** The resonance frequencies for even mode according to physical length of W_1. **(b)** The resonance frequencies for odd mode according to physical length W_1. **(c)** The resonance frequencies for even mode according to L_{10} parameter. **(d)** The resonance frequencies for odd mode according to L_{10} parameter

By increasing L10, the even and odd mode resonance frequencies are moved towards lower frequencies. As observed in Figs. 4(a) and 4(b), the values of even and odd resonance frequencies in the pass-band are independent of W3 and for high frequency, for the physical length of W3 (W3=0.8, 1, and 1.2mm), the resonance frequencies can shift towards upper frequency. Similarly, as is shown in Figs. 4(c) and 4(d), L4 can be used to adjust pass-band and the center frequency the values of the even mode and odd resonance frequencies in pass-band are independent of L4 and the resonance frequencies in stop-band for larger values of L4 (L4=1.7, 2.9 and 4.1mm) can also move towards upper frequency.

As is shown in Fig. 5, W1 is used to adjust pass-band and the center frequency. Similarly, as is shown in Fig. 6, L10 can be used to adjust pass-band and the center frequency. W3 and other interdigital line are used to move spurious resonance frequencies to high frequency and finally suppressed with the proper design and use of cell attenuator (the open-ended stub in Fig. 1). The simulated S-parameters of the BPF before employing cell attenuator is shown in Fig. 7. As can be seen, unwanted harmonics are observed in the stop-band, and the cell attenuator can be used to develop stop-band. It is necessary to know the accuracy of the level in stop-band. In order to reduce the signal level, attenuators dissipate the unwanted signal. For many applications where signal levels are high, it is necessary to ensure that the cell attenuator will be able to remove unwanted signal.

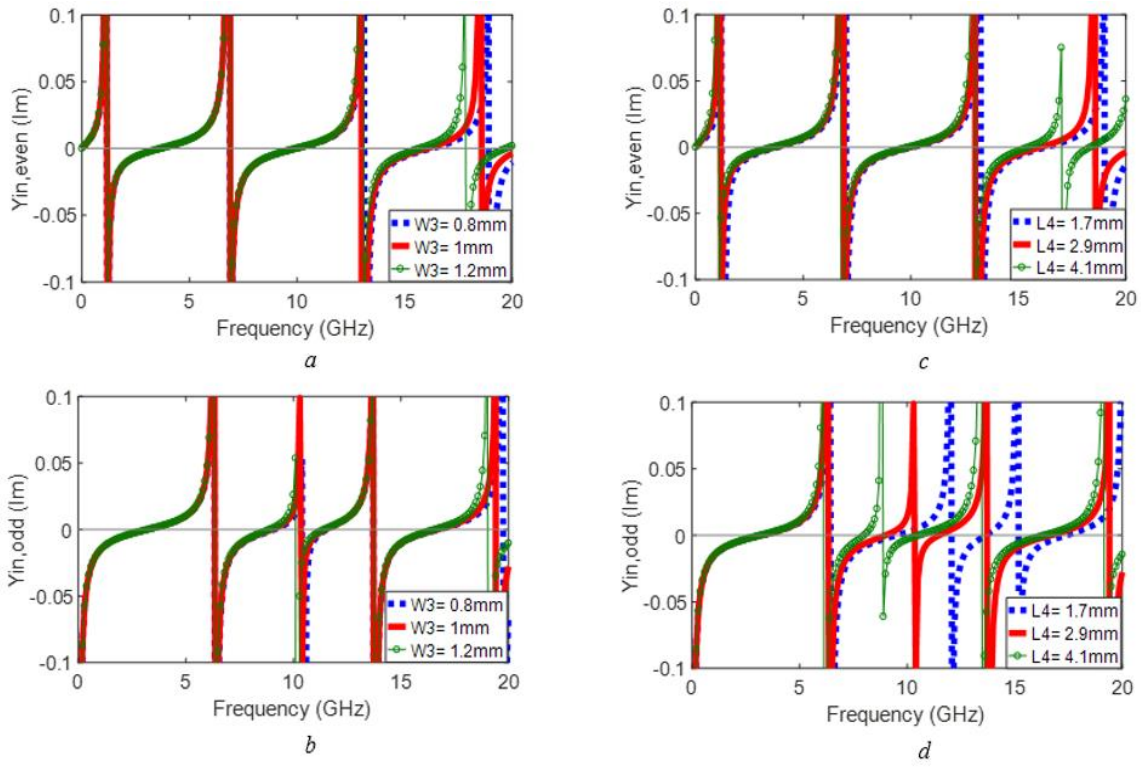

Fig. 4. The odd and even modes analysis. **(a)** The resonance frequencies for even mode according to W_3 parameter (correspond to the electrical length θ_3). **(b)** The resonance frequencies odd mode resonance frequencies according to W_3 parameter. **(c)** The resonance frequencies for even mode according to L_4 parameter (correspond to the width of microstrip line). **(d)** The resonance frequencies for odd mode according to L_4 parameter.

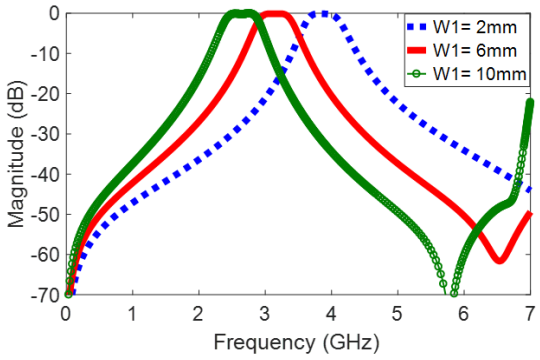

Fig. 5. Simulated S_{21} (transmission parameter) for different W_1 parameter

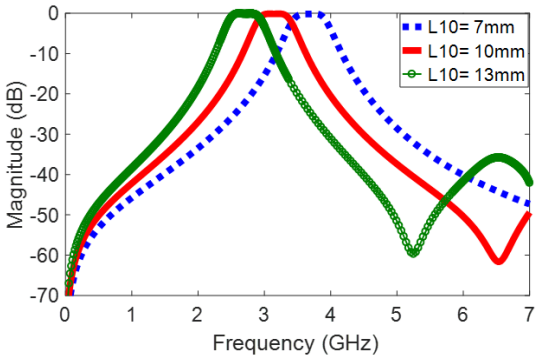

Fig. 6. Simulated S_{21} (transmission parameter) for different L_{10} parameter.

III. FABRICATION AND RESULTS

Fig. 8 shows that the fabricated filter exhibits a flat group delay (less than 1ns in pass-band). Fig. 9 shows the photograph of the proposed BPF. The substrate used here has a relative dielectric constant of 2.2 and a thickness of 0.508 mm, and a loss tangent of 0.0009. Fig. 9 also illustrates the simulated and measured results of the designed BPF. The simulations are carried out using ADS Momentum and HFSS software. An N5230A network analyzer is used to measure the S-parameter of the filter. As is

shown in Fig. 9, the simulation results and the measured values are in relative good agreement.

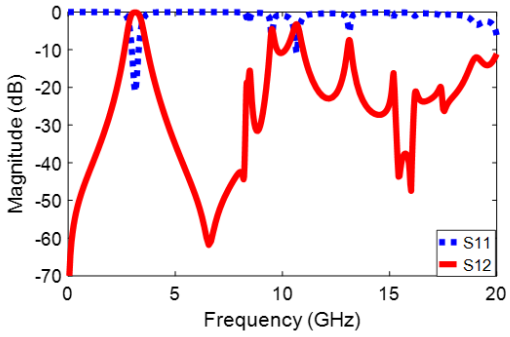

Fig. 7. The simulated S-parameters of the BPF before adding LPF

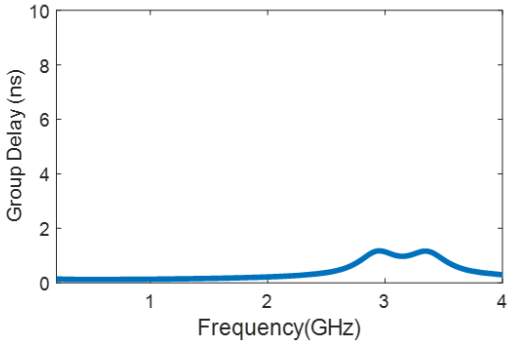

Fig. 8. The Measured group delays.

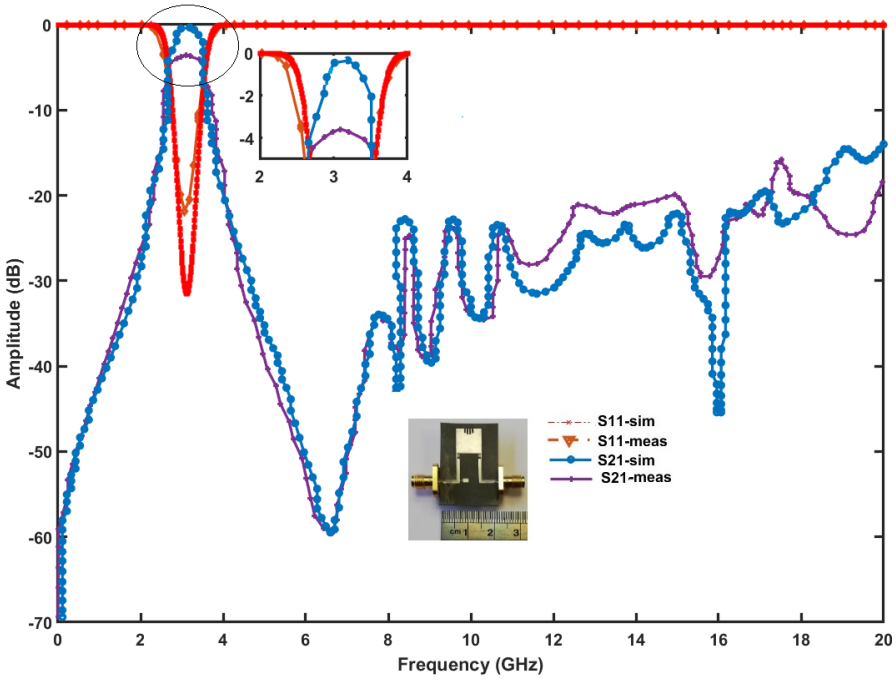

Fig. 9. Simulated, measured S-parameters and the photograph of the BPF.

The insertion loss has a minimum of 0.1 dB and 3.715 dB in the pass-band (at simulation and measurement, respectively), 3dB fractional bandwidth of 25%, the center frequency of 3.095 GHz that can change from 2.4 to 4GHz, wide stop-band from 3.7 GHz to 17 GHz, sharp transition band and the size of 21× 22 mm2. The difference between simulation and measurement results is inevitable due to the process of fabrication and test conditions.

Table 2 summarizes the performance comparison between the related work in the literature and the proposed BPF. From this table, it can be concluded that the proposed bandpass filter has improved in-band and out of band performances.

Table II. Performance comparison

Ref.	$f_0(GHz)$	IL (dB)	3 dB FBW	Sharp roll off
[11]	2.45	0.6	22%	Yes
[18]	2.45	5.5	1.6%	No
[19]	5.5	4.76	14.8%	No
[20]	2	3.9	11%	No
[21]	2.78	4.2	23.4%	Yes
This work	3.095	3.715	25%	Yes

IV. CONCLUSION

A new microstrip BPF consists of parallel coupled lines, the modified 3-section SIR and, a LPF is designed, analyzed, and tested. The fabricated filter has the merits of compact size, low insertion loss and, wide stop-band. The center frequency can change from 2.4 to 4GHz, while the bandwidth remains fix. Overall, this Filter has excellent performance compared to the previous works, so, it is suitable for wireless communications and radar applications.

REFERENCES

[1] J.-S. Hong and M. J. Lancaster, *Microstrip Filters for RF/Microwave Application*, New York, NY, USA: Wiley, 2001.

[2] F.-C Chen, J.-M. Qiu, H.-T. Hu, Q.-X. Chu, and M.J. Lancaster, "Design of microstrip lowpass-bandpass triplexer with high isolation," *IEEE Microwave and Wireless Components Letters*, vol. 25, no. 12, pp. 805–807, Dec. 2015.

[3] K.M. Shum, T.T. Mo, Q. Xue, and C.H. Chan, "A compact bandpass filter with two tuning transmission zeros using a CMRC resonator," *IEEE Trans. Microwave Theory and Techniques*, vol. 53, no. 3, pp. 895–900, Mar. 2005.

[4] S.-C. Lin, Y.S. Lin, and C.H. Chen, "Extended-stop-band bandpass filter using both half- and quarter-wavelength resonators," *IEEE Microwave and Wireless Components Letters*, vol. 16, no. 1, pp. 43–45, Jan. 2006.

[5] J.-K. Xiao, N. Zhang, J.-G. Ma,, and J.-S. Hong, "Microstrip/coplanar waveguide hybrid bandpass filter with electromagnetic coupling," *IEEE Microwave and Wireless Components Letters*, vol. 26, no. 10, pp. 780–782, Sep. 2016.

[6] X. Huang, L. Zhu, Q. Feng, Q. Xiang, and D. Jia, "Tunable bandpass filter with independently controllable dual pass-bands," *IEEE Trans. Microwave Theory and Techniques*, vol. 61, no. 9, pp. 3200–3208, Aug. 2013.

[7] R. Gomez-Garcia, A.C. Guyette, D.Psychogiou, E.J. Naglich, and D. Peroulis, "Quasi-elliptic multi-band filters with center-frequency and bandwidth tenability," *IEEE Microwave and Wireless Components Letters*, vol. 26, no. 3, pp. 192–194, Feb. 2016.

[8] H. Xu, J. Wang, L. Zhu, F. Huang, and W. Wu, "Design of a dual-mode balun bandpass filter with high selectivity," *IEEE Microwave and Wireless Components Letters*, vol. 28, no. 1, pp. 22–24, Dec. 2018.

[9] F. Farzami, S. Khaledian, A. C. Stutts, B. Smida, and D. Erricolo, "Embedded Split Ring Resonator Tunable Notch Band Filter in Microstrip Transmission Lines," IEEE Access, vol. 10, pp. 37294-37304, 2022.

[10] Y. Rao, H. J. Qian, B. Yang, R. Gómez-García, and X. Luo, "Dual-band bandpass filter and filtering power divider with ultra-wide upper stop-band using hybrid microstrip/DGS dual-resonance cells," IEEE Access, vol. 8, pp. 23624-23637, 2020.

[11] X. Wu, Y. Li, and X. Liu, "High-order dual-port quasi-absorptive microstrip coupled-line bandpass filters," IEEE Trans. Microwave Theory and Techniques, vol. 68, no. 4, pp. 1462-1475, April 2020.

[12] K.-D. Xu, S. Lu, Y.-J. Guo, and Q. Chen, "Quasi-reflectionless filters using simple coupled line and T-shaped microstrip structures," IEEE Journal of Radio Frequency Identification, vol. 6, pp. 54-63, 2021.

[13] Z. Shaterian and M. Mrozowski, "A Multifunctional Microwave Filter/Sensor Component Using a Split Ring Resonator Loaded Transmission Line," I*EEE Microwave and Wireless Components Letters*, vol. 33, no. 2, pp. 220 - 223, Feb. 2023.

[14] M. Nosrati and M. Daneshmand, "Compact microstrip ultra-wideband double/single notch band bandpass filter based on wave's cancellation theory," *IET Microwave, Antennas and Propagation*, vol. 12, no. 6, pp. 862–868, Jul. 2012.

[15] F. Wei, Q.Y. Wu, X.W. Shi, and L. Chen, "Compact UWB bandpass filter with dual notched bands based on SCRLH resonator," *IEEE Microwave and Wireless Components Letters*, vol. 21, no. 1, pp. 28–30, Nov. 2011.

[16] E. Djoumessi, , M. Chaker, and K. Wu, "Varactor-tuned quarter-wavelength dual-bandpass filter," *IET Microwaves, Antennas & Propagation*, vol. 3, no. 1, p. 117-124, Jan. 2009.

[17] A. Vaezi and and F. Geran Gharaklili, "Synthesis and design of an LPF with wide-stop band and high rejection level," *AEU - International Journal of Electronics and Communications*, vol. 95, pp. 139–145, Oct. 2018.

[18] E.-Y. Jung and H.-Y. Hwang, "A balun-BPF using a dual mode ring resonator," *IEEE Microwave and Wireless Components Letters*, vol. 17, no. 9, pp. 652–654, Aug. 2007.

[19] J.-X. Xu, X.Y. Zhang, and X.-L. Zhao, "Compact LTCC balun with bandpass response based on marchand balun," *IEEE Microwave and Wireless Components Letters*, vol. 26, no. 7, pp. 493–495, Jun. 2016.

[20] J. Wang, F. Huang, L. Zhu, C. Cai, and W. Wu, "Study of a new planar-type balun topology for application in the design of balun bandpass filters," *IEEE Trans. Microwave Theory and Techniques*, vol. 64, no. 9, pp. 2824–2832, Aug. 2016.

[21] H. Xu, J. Wang, L. Zhu, F. Huang, and W. Wu "Design of a dual-mode balun bandpass filter with high selectivity," *IEEE Microwave and Wireless Components Letters*, vol. 28, no. 1, pp. 22–24, Jan. 2018.